Auto-regressive modeling of the shadowing for RSS mobile tracking

Hadi Noureddine*†, Nicolas Gresset*, Damien Castelain*, Ramesh Pyndiah†
*Mitsubishi Electric R&D Centre Europe, France
†Telecom Bretagne, France

***Abstract*—In this paper, we consider the tracking of mobile terminals based on the received signal strength (RSS) measured from several base stations. The spatial correlation of the random shadowing is exploited in order to improve the position tracking. We define an auto-regressive (AR) model of the temporal evolution of the shadowing. This model allows for performing a joint tracking of the position and the shadowing by applying a Rao-Blackwellized (RB) particle filter approximating the posterior probability distributions numerically. The simulation results show that the tracking can be improved by considering sufficiently high auto-regressive orders.**

I. Introduction

Navigation tasks and fleet management are among the first applications of positioning and tracking. These applications have been diversified to include geo-localization of emergency calls, network control, and a variety of location-based services.

Wireless networks have been considered as a supplement or an alternative to the GPS solution for localizing mobile terminals. Several position dependent properties of the radio signals can be exploited and several solutions have been developed [1].

The position tracking relies on the measurements obtained from the radio signals or from the outputs of an inertial navigation system (INS), and on a displacement model. It performs the estimation of the hidden state vector composed of the position and other parameters of interest.

In this paper, we focus on mobile tracking using the RSS measurements. The obstacles in the propagation path between a user equipment (UE) and a base station (BS) cause attenuations in the form of slow fading or shadowing. The shadowing is usually assumed to follow a spatially correlated log-normal distribution [2][3]. As the UE moves, the spatial correlation is transformed into a temporal one.

Several RSS-based algorithms have been proposed in order to improve the position tracking in presence of random shadowing. In [4], a prediction of the shadowing, modeled by a first order auto-regressive Gaussian process, is used along with the RSS measurements for estimating position. This solution is sub-optimal, and can be improved by using a probabilistic approach.

Thus, our solution is based on Bayesian filtering, which efficiently exploits the incoming measurements by recursively updating the posterior probability distribution. The update is performed by taking the shadowing as a part of the state vector, whose stochastic process is no more Markovian. The transition equations of this process are obtained by an auto-regressive modeling of the shadowing evolution.

As a remark, an alternative approach was used in a general context in [5], where the shadowing was considered as a measurement noise and the temporal correlation was accounted for in evaluating the likelihood function.

Recursive Monte Carlo methods, also known as particle filters [6][7], allow for approximating the probability density functions which are analytically untraceable because of the non-linearity of the AR model and the RSS measurements with respect to the position. More specifically, a Rao-Blackwellized particle filter will be implemented where the part of the state vector consisting of the position and its derivatives is represented by particles and the shadowing part is tracked by means of a Kalman filter. This solution has the advantage of reducing the needed amount of particles.

This paper is organized as follows. In section II, the transition model describing the evolution of the state vector and the observation model are presented. In section III, we introduce the auto-regressive modeling of the shadowing evolution. The RB particle filter for solving the tracking problem is presented in section IV. In section V, we show that for a particular case of a collinear trajectory and under an exponential correlation function, the shadowing follows a first order $AR(1)$ model. Simulation results and conclusions are presented in sections VI and VII, respectively.

II. System model

In this section, we describe the transition model of the hidden state vector and the observation model. They allow for computing the a priori and likelihood probabilities in the Bayesian filtering processing, respectively.

A. Transition model

We define the kinematic vector $\mathbf{c}_k$ at time kT, where $k \in \mathbb{N}$ and T is a time step, comprising the UE position $\mathbf{x}_k = [x_k, y_k]^T$ and other kinematic parameters (e.g. velocity). This vector is issued from a known Markov process of transition probability $p(\mathbf{c}_k|\mathbf{c}_{k-1})$ and initial distribution $p(\mathbf{c}_0)$.

We denote $\Omega_k = [\epsilon_1(\mathbf{x}_k), \cdots, \epsilon_{N_{BS}}(\mathbf{x}_k)]^T$, where $\epsilon_i(\mathbf{x}_k)$ is the shadowing value in decibel (dB) corresponding to the i-th base station out of N_{BS}. The shadowing is assumed invariant in time for a fixed position.

The state vector $\mathbf{s}_k$ is defined by

$$\mathbf{s}_k = [\mathbf{c}_k^T, \Omega_k^T]^T. \quad (1)$$

We can decompose the transition equation as

$$p(\mathbf{s}_k|\mathbf{s}_{0:k-1}) = p(\mathbf{c}_k|\mathbf{c}_{k-1})p(\Omega_k|\mathbf{x}_{0:k}, \Omega_{0:k-1}) \quad (2)$$

where $\mathbf{s}_{0:k-1} = [\mathbf{s}_0^T, \cdots, \mathbf{s}_{k-1}^T]^T$, $\mathbf{x}_{0:k}$ and $\Omega_{0:k-1}$ being defined accordingly. In section III, we show that Ω_k is represented by an AR model, which allows for computing $p(\Omega_k|\mathbf{x}_{0:k}, \Omega_{0:k-1})$.

B. Observation model

At time kT, the UE makes RSS measurements $\mathbf{y}_k(dB)$ from l_k signals sent by multi-sectors base stations, the sectors being created by limited-interference antenna diagrams. The measurements vector is equal to

$$\mathbf{y}_k = \mathbf{f}_k(\mathbf{x}_k) + \mathbf{J}_k\Omega_k + \mathbf{n}_k \quad (3)$$

where $\mathbf{f}_k$ is a deterministic empirical function of the path loss that takes the antenna diagrams into account; $\mathbf{J}_k$ is an $l_k \times N_{BS}$ matrix where $\mathbf{J}_k(i,j) = 1$ if the i-th measurement is made on the j-th base station and 0 elsewhere; and $\mathbf{n}_k$ is a Gaussian error that arises from moving obstacles or non-shadowing losses and is considered to be white with respect to the time domain.

III. Autoregressive shadowing model

In this section, we describe the evolution of the shadowing as an AR model in the case of a single base station, and then make the generalization for multiple base stations.

A. Shadowing AR model for a single base station

Here, we focus on the case where a single base station lies in the system. For clarity reasons, the subscript of ϵ is dropped in this section.

The correlation of the shadowing at times lT and mT is

$$E\{\epsilon(\mathbf{x}_l)\epsilon(\mathbf{x}_m)\} = \sigma_{sh}^2\rho(\|\mathbf{x}_l - \mathbf{x}_m\|) \quad (4)$$

where ρ is an isotropic correlation function, i.e., depends only on the distance between the two positions. By definition $\rho(0) = 1$.

Knowing the positions $\mathbf{x}_{0:k}$ and prior to any observation, $[\epsilon(\mathbf{x}_0), \cdots, \epsilon(\mathbf{x}_k)]^T$ is a zero mean Gaussian distributed vector of covariance matrix $\mathbf{R}_k$, with $\mathbf{R}_k(l,m) = \sigma_{sh}^2\rho(\|\mathbf{x}_l - \mathbf{x}_m\|)$. We write $\mathbf{R}_k$ as follows:

$$\mathbf{R}_k = \begin{bmatrix} \mathbf{R}_{k-1} & \mathbf{r}_k \\ \mathbf{r}_k^T & \sigma_{sh}^2 \end{bmatrix} \quad (5)$$

where the vector $\mathbf{r}_k = E\{[\epsilon(\mathbf{x}_0), \cdots, \epsilon(\mathbf{x}_{k-1})]^T\epsilon(\mathbf{x}_k)\}$.

Furthermore, $p(\epsilon(\mathbf{x}_k)|\mathbf{x}_{0:k}, \epsilon(\mathbf{x}_0), \cdots, \epsilon(\mathbf{x}_{k-1}))$ being a Gaussian distribution, the process $\epsilon(\mathbf{x}_k)$ can be represented by an order-k AR model $AR(k)$

$$\epsilon(\mathbf{x}_k) = \mathbf{a}_k^T[\epsilon(\mathbf{x}_0), \cdots, \epsilon(\mathbf{x}_{k-1})]^T + \theta_k \quad (6)$$

where

$$\mathbf{a}_k = \mathbf{R}_{k-1}^{-1}\mathbf{r}_k \quad (7)$$

and θ_k is a zero mean Gaussian variable of variance $\sigma_{\theta_k}^2$:

$$\sigma_{\theta_k}^2 = \sigma_{sh}^2 - \mathbf{r}_k^T\mathbf{R}_{k-1}^{-1}\mathbf{r}_k. \quad (8)$$

In order to take all the previous states into account, the order of the AR model increases with time. The matrix inversion $\mathbf{R}_k^{-1}$ can be computed recursively with low complexity by using

$$\begin{aligned}\mathbf{R}_k^{-1} &= \begin{bmatrix} \mathbf{I} & -\mathbf{R}_{k-1}^{-1}\mathbf{r}_k \\ \mathbf{0} & 1 \end{bmatrix}\begin{bmatrix} \mathbf{R}_{k-1}^{-1} & \mathbf{0} \\ \mathbf{0} & 1/\sigma_{\theta_k}^2 \end{bmatrix} \\ &\quad \times \begin{bmatrix} \mathbf{I} & \mathbf{0} \\ -\mathbf{r}_k^T\mathbf{R}_{k-1}^{-1} & 1 \end{bmatrix}. \end{aligned} \quad (9)$$

As a remark, the order of the AR process can be limited to the $p < (k+1)$ previous states, $\mathbf{R}_k^{-1}$ being replaced by the inverse of the $p \times p$ lower right submatrix of $\mathbf{R}_k$ or by the Schur's complement of the $(k-p+1) \times (k-p+1)$ upper left submatrix of $\mathbf{R}_k^{-1}$. Thus, if a sliding window approach of depth p is considered, the Schur's complement is of low complexity as it doesn't need any matrix inversion.

B. Shadowing AR model for multiple base stations

The shadowings of different base stations are cross-correlated [8]. By considering a constant correlation coefficient, we can model the shadowing of the i-th base station by a sum of two i.i.d. Gaussian random fields:

$$\epsilon_i(\mathbf{x}_k) = \alpha GF_i(\mathbf{x}_k) + \beta GF_c(\mathbf{x}_k) \quad (10)$$

where $\alpha^2 + \beta^2 = \sigma_{sh}^2$ and GF_c is common for all base stations. The following cross-correlation properties are assumed:

$$\begin{aligned} E\{GF_i(\mathbf{x}_l)GF_j(\mathbf{x}_m)\} &= 0. \\ E\{GF_i(\mathbf{x}_l)GF_i(\mathbf{x}_m)\} &= \rho(\|\mathbf{x}_l - \mathbf{x}_m\|). \\ E\{\epsilon_i(\mathbf{x}_l)\epsilon_j(\mathbf{x}_m)\} &= \beta^2\rho(\|\mathbf{x}_l - \mathbf{x}_m\|). \end{aligned}$$

Prior to any observation, $\Omega_{0:k}$ is a zero mean Gaussian distributed vector of covariance matrix $\mathbf{P}_k$ equal to

$$\mathbf{P}_k = \begin{bmatrix} \mathbf{P}_{k-1} & \mathbf{T}_k \\ \mathbf{T}_k^T & \sigma_{sh}^2\mathbf{Z} \end{bmatrix} \quad (11)$$

where $\mathbf{T}_k = E\{\Omega_{0:k-1}\Omega_k^T\}$ and $\mathbf{Z}$ is the $N_{BS} \times N_{BS}$ matrix defined by

$$\mathbf{Z} = \begin{bmatrix} 1 & \beta^2/\sigma_{sh}^2 & \cdots & \beta^2/\sigma_{sh}^2 \\ \beta^2/\sigma_{sh}^2 & \ddots & \ddots & \vdots \\ \vdots & \ddots & \ddots & \beta^2/\sigma_{sh}^2 \\ \beta^2/\sigma_{sh}^2 & \cdots & \beta^2/\sigma_{sh}^2 & 1 \end{bmatrix}.$$

The Gaussian process Ω_k can be represented by the $AR(k)$ model

$$\Omega_k = \mathbf{A}_k^T\Omega_{0:k-1} + \Theta_k \quad (12)$$

where

$$\mathbf{A}_k = \mathbf{P}_{k-1}^{-1}\mathbf{T}_k \quad (13)$$

and Θ_k is a zero mean Gaussian distributed vector of covariance matrix $\mathbf{Q}_k$. Thus, the Gaussian distribution $p(\Omega_k|\mathbf{x}_{0:k}, \Omega_{0:k-1})$, which is needed in order to determine the transition equation (2), has a mean $\mathbf{A}_k^T\Omega_{0:k-1}$ and a covariance matrix $\mathbf{Q}_k$.

From (5) and (11), $\mathbf{P}_k = \mathbf{R}_k \otimes \mathbf{Z}$ where $\otimes$ denotes the Kronecker product, which allows for computing $\mathbf{P}_k^{-1} = \mathbf{R}_k^{-1} \otimes \mathbf{Z}^{-1}$. Thus, the matrix $\mathbf{A}_k$ defined in (13) can be computed with low complexity

$$\begin{aligned}\mathbf{A}_k &= \left(\mathbf{R}_{k-1}^{-1} \otimes \mathbf{Z}^{-1}\right) \times (\mathbf{r}_k \otimes \mathbf{Z}) \\ &= \mathbf{a}_k \otimes \mathbf{I}(N_{BS}) \end{aligned} \quad (14)$$

where $\mathbf{I}(N_{BS})$ is the identity matrix of rank N_{BS}. Similarly, the covariance matrix $\mathbf{Q}_k$ of Θ_k is equal to

$$\mathbf{Q}_k = \sigma_{sh}^2 \mathbf{Z} - \mathbf{T}_k^T \mathbf{P}_{k-1}^{-1} \mathbf{P}_k = \sigma_{\theta_k}^2 \mathbf{Z}. \quad (15)$$

Thus, the transition probabilities of the shadowing process can be computed with low complexity.

IV. Bayesian Tracking implementation

In this section, we present the Bayesian filtering adapted to the AR model of the system and using Rao-Blackwellization.

A. Bayesian filtering

A Bayesian filtering consists of determining recursively in time $p(\mathbf{s}_{0:k}|\mathbf{y}_{1:k})$ in order to apply a Bayesian estimator, e.g. the MMSE estimator:

$$\hat{\mathbf{s}}_k = \int \mathbf{s}_k p(\mathbf{s}_{0:k}|\mathbf{y}_{1:k}) \mathrm{d}\mathbf{s}_{0:k} \quad (16)$$

where $p(\mathbf{s}_{0:k}|\mathbf{y}_{1:k})$ is computed recursively according to

$$p(\mathbf{s}_{0:k}|\mathbf{y}_{1:k}) = p(\mathbf{s}_{0:k-1}|\mathbf{y}_{1:k-1}) \frac{p(\mathbf{s}_k|\mathbf{s}_{0:k-1}) p(\mathbf{y}_k|\mathbf{s}_k)}{p(\mathbf{y}_k|\mathbf{y}_{1:k-1})}. \quad (17)$$

When an order-p AR process is considered, $p(\mathbf{s}_k|\mathbf{s}_{0:k-1})$ is replaced by $p(\mathbf{s}_k|\mathbf{s}_{k-p:k-1})$.

B. Rao-Blackwellized particle filter

The shadowing evolution equation (12) and the measurement equation (3) are non-linear with respect to $\mathbf{x}_k$ making the posterior density (17) untraceable analytically. Particle filters allows for computing numerically the solutions, with a complexity drawback. Indeed, the number of particles usually must increase exponentially with the dimension of the state vector. In our case, the dimension of the state vector is increasing with the number of shadowing components used in the tracking process.

We can remark that, conditionally on the knowledge of $\mathbf{x}_{0:k}$, equations (12) and (3) are linear with respect to Ω_k, which can be tracked by a Kalman filter. Thus, we can reduce the number of particles and limit the complexity of the filter by applying a Rao-Blackwellization. This consists of computing the posterior of a subset of the state vector analytically, in our case with the Kalman filter.

At time $(k-1)T$, if we assume that $p(\mathbf{c}_{0:k-1}|\mathbf{y}_{1:k-1})$ is approximated by the set of weighted particles $\left\{w_{k-1}^i, \mathbf{c}_{0:k-1}^i\right\}_{i=1}^N$ and that the Gaussian distribution $p(\Omega_{0:k-1}|\mathbf{x}_{0:k-1}^i, \mathbf{y}_{1:k-1}) = N(\mathbf{M}_{k-1}^i, \mathbf{C}_{k-1}^i)$ is known, then the posterior distribution $p(\mathbf{s}_{0:k-1}|\mathbf{y}_{1:k-1})$ can be expressed as

$$\begin{aligned} &p(\mathbf{s}_{0:k-1}|\mathbf{y}_{1:k-1}) \\ &\quad = p(\Omega_{0:k-1}|\mathbf{x}_{0:k-1}, \mathbf{y}_{1:k-1}) p(\mathbf{c}_{0:k-1}|\mathbf{y}_{1:k-1}) \\ &\quad \approx \textstyle\sum_i w_{k-1}^i N(\mathbf{M}_{k-1}^i, \mathbf{C}_{k-1}^i) \delta(\mathbf{c}_{0:k-1}, \mathbf{c}_{0:k-1}^i) \end{aligned} \quad (18)$$

where δ is the Kronecker delta function.

The posterior distribution $p(\mathbf{s}_{0:k}|\mathbf{y}_{1:k})$ at time kT can be obtained in three steps.

1) Prediction step: The predictive distribution $p(\mathbf{s}_{0:k}|\mathbf{y}_{1:k-1})$ can be written as

$$\begin{aligned} &p(\mathbf{s}_{0:k}|\mathbf{y}_{1:k-1}) \\ &\quad = p(\Omega_{0:k}|\mathbf{x}_{0:k}, \mathbf{y}_{1:k-1}) p(\mathbf{c}_{0:k}|\mathbf{y}_{1:k-1}) \\ &\quad \approx \textstyle\sum_i w_{k-1}^i p(\Omega_k|\mathbf{x}_k, \mathbf{x}_{0:k-1}^i, \Omega_{0:k-1}) N(\mathbf{M}_{k-1}^i, \mathbf{C}_{k-1}^i) \times \\ &\qquad p(\mathbf{c}_k|\mathbf{c}_{k-1}^i) \delta(\mathbf{c}_{0:k-1}, \mathbf{c}_{0:k-1}^i). \end{aligned} \quad (19)$$

A Monte Carlo approximation of this distribution is

$$\begin{aligned} p(\mathbf{s}_{0:k}|\mathbf{y}_{1:k-1}) \approx \textstyle\sum_i w_{k-1}^i N(\mathbf{M}_{k|k-1}^i, \mathbf{C}_{k|k-1}^i) \times \\ \delta(\mathbf{c}_{0:k}, \mathbf{c}_{0:k}^i). \end{aligned} \quad (20)$$

where $\mathbf{c}_k^i$ is drawn from $p(\mathbf{c}_k|\mathbf{c}_{k-1}^i)$,

$$\mathbf{M}_{k|k-1}^i = \begin{bmatrix} \mathbf{M}_{k-1}^i \\ (\mathbf{A}_k^i)^T \mathbf{M}_{k-1}^i \end{bmatrix} \quad (21)$$

and

$$\mathbf{C}_{k|k-1}^i = \begin{bmatrix} \mathbf{C}_{k-1}^i & \mathbf{C}_{k-1}^i \mathbf{A}_k^i \\ (\mathbf{A}_k^i)^T \mathbf{C}_{k-1}^i & (\mathbf{A}_k^i)^T \mathbf{C}_{k-1}^i \mathbf{A}_k^i + \mathbf{Q}_k^i \end{bmatrix}. \quad (22)$$

$\mathbf{A}_k^i$ and $\mathbf{Q}_k^i$ are obtained from equations (13) and (15) for the trajectory $\mathbf{x}_{0:k}^i$.

2) Correction step: In this step, the observation $\mathbf{y}_k$ is used to compute $p(\mathbf{s}_{0:k}|\mathbf{y}_{1:k})$ by updating $p(\mathbf{s}_{0:k}|\mathbf{y}_{1:k-1})$.

The observation equation (3) is re-written as follows:

$$\mathbf{y}_k = \mathbf{f}_k(\mathbf{x}_k) + \mathbf{H}_k \Omega_{0:k} + \mathbf{n}_k \quad (23)$$

where $\mathbf{H}_k = [\mathbf{0}, \mathbf{J}_k]$ of size $l_k \times (k+1)N_{BS}$.

Before being normalized, the weights are updated by

$$w_k^i \propto w_{k-1}^i p(\mathbf{y}_k|\mathbf{x}_{0:k}^i, \mathbf{y}_{1:k-1}) \quad (24)$$

where $p(\mathbf{y}_k|\mathbf{x}_{0:k}^i, \mathbf{y}_{1:k-1})$ is a Gaussian distribution of mean $\mathbf{f}_k(\mathbf{x}_k^i) + \mathbf{H}_k \mathbf{M}_{k|k-1}^i$ and covariance $\mathbf{H}_k \mathbf{C}_{k|k-1}^i \mathbf{H}_k^T + E\{\mathbf{n}_k \mathbf{n}_k^T\}$.

The vector $\mathbf{M}_k^i$ and matrix $\mathbf{C}_k^i$ are obtained by means of a Kalman filter described as follows:

- Kalman gain:

$$\mathbf{K}_k^i = \mathbf{C}_{k|k-1}^i \mathbf{H}_k^T (\mathbf{H}_k \mathbf{C}_{k|k-1}^i \mathbf{H}_k^T + E\{\mathbf{n}_k \mathbf{n}_k^T\})^{-1} \quad (25)$$

- Mean correction:

$$\mathbf{M}_k^i = \mathbf{M}_{k|k-1}^i + \mathbf{K}_k^i (\mathbf{y}_k - \mathbf{f}_k(\mathbf{x}_k^i) - \mathbf{H}_k \mathbf{M}_{k|k-1}^i) \quad (26)$$

- Covariance correction:

$$\mathbf{C}_k^i = \left(\mathbf{I}((k+1)N_{BS}) - \mathbf{K}_k^i \mathbf{H}_k\right) \mathbf{C}_{k|k-1}^i \quad (27)$$

When an order-p AR model is considered, it is sufficient to store $\mathbf{c}_{k-p+1:k}^i$, the last p elements of $\mathbf{M}_k^i$ and the $p \times p$ lower right submatrix of $\mathbf{C}_k^i$.

3) Resampling step: In order to avoid the weights degeneracy [6] due to the increase of the variance of the set $\left\{w_k^i\right\}_{i=1}^N$, a resampling step is performed. Thus, some trajectories of weak weights are eliminated and some of strong weights repeated. We execute this step when the effective number of particles $N_{eff} = 1/\sum_i (w_k^i)^2$ falls below a threshold. Unfortunately, resampling causes a depletion of the history due to the common past shared by some trajectories [9].

As a remark, when one small region is visited several times during a window time fitting the AR model order, the shadowings observations associated to this region are highly correlated. The performance might be decreased if the number of remaining distinct particles is not sufficient.

V. Special case of collinear trajectories

In this section, we consider collinear trajectories for the sake of illustration. In practice, this allows for using a map-restricted trajectory along with the presented technology. For example, train geo-location, or car geo-location are examples of applications. Of course, when a crossroad approaches, all possible trajectories can be taken into account independently in the particle filter, and selected according to the maximal weights after crossing the intersection.

For Gaussian vectors, the precision matrix, i.e., the inverse of the covariance matrix, explicitly contains the information about the conditional independence of their components [10]. Let $\mathbf{v} = [v_1, \cdots, v_n]^T$ be a Gaussian vector of precision matrix Λ, then

$$v_i \perp v_j | \mathbf{v}_{\_i,j} \quad \Leftrightarrow \quad \Lambda_{i,j} = 0$$

where $\perp$ denotes the independence, and $\mathbf{v}_{\_i,j}$ is $\mathbf{v}$ without v_i and v_j.

Consider a set of L collinear points located on the x-axis and verifying $x_{j+1} > x_j$ as shown in Fig. 1.

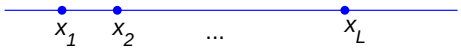

Fig. 1. A trajectory of collinear points.

Consider also an exponential correlation function of the form

$$\rho(\|\mathbf{x}_l - \mathbf{x}_m\|) = e^{-\gamma \|\mathbf{x}_l - \mathbf{x}_m\|} \tag{28}$$

where γ is a constant. In this case, it can be shown that the precision matrix $\mathbf{R}_L^{-1}$ of $[\epsilon(\mathbf{x}_0), \cdots, \epsilon(\mathbf{x}_L)]^T$ is tridiagonal.

$$\mathbf{R}_L^{-1} = \begin{bmatrix} a_1 & b_1 & 0 & \cdots & 0 \\ b_1 & a_2 & \ddots & \ddots & \vdots \\ 0 & \ddots & \ddots & \ddots & 0 \\ \vdots & \ddots & \ddots & a_{L-1} & b_{L-1} \\ 0 & \cdots & 0 & b_{L-1} & a_L \end{bmatrix} \tag{29}$$

As a result, the Gaussian process $\epsilon(\mathbf{x}_L)$ is an $AR(1)$ process. This can be deduced by looking at the last row of $\mathbf{R}_L^{-1}$ which has only two nonzero entries.

VI. Simulations

In this section we introduce the transition and the observation model scenarios assumed for the computer simulations and show the results. We show the robustness of the algorithm for a collinear trajectory with a varying speed. In order to illustrate the benefit taken from higher AR model orders, we also consider the case of a U-turn.

The motion of the UE is modeled by a simple linear Markov process. The kinematic vector is $\mathbf{c}_k = [x_k, \dot{x}_k, y_k, \dot{y}_k]^T$ where $[\dot{x}_k, \dot{y}_k]^T$ is the velocity vector. $\mathbf{c}_k$ evolves according to the following difference equation:

$$\mathbf{c}_k = \begin{bmatrix} 1 & T & 0 & 0 \\ 0 & 1 & 0 & 0 \\ 0 & 0 & 1 & T \\ 0 & 0 & 0 & 1 \end{bmatrix} \mathbf{c}_{k-1} + \begin{bmatrix} 0 & 0 \\ T & 0 \\ 0 & 0 \\ 0 & T \end{bmatrix} (\mathbf{q}_{k-1} + \mathbf{e}_{k-1}) \tag{30}$$

where we assume that $\mathbf{q}_{k-1} = [q_{x,k-1}, q_{y,k-1}]^T$ is the acceleration vector provided by an accelerometer and $\mathbf{e}_{k-1}$ is a Gaussian distributed vector that accounts for the acceleration estimation errors. We take the covariance of $\mathbf{e}_{k-1}$ equal to $(0.5m/s^2)^2\mathbf{I}(2)$. We perform tracking with a map constraint, where the trajectory belongs to a straight road with two lanes.

We use the model in (30) for tracking, while the trajectories are generated according to the model developed in [11] which takes into account a dynamic model of the vehicle, the driver's control decisions and the map of lanes. We consider the two trajectories depicted in Fig. 2. Trajectory 1 is a straight line with an average velocity of $57km/h$ and a maximum velocity of $72km/h$. Notice that the vehicle is accelerating at the beginning. Trajectory 2 contains a turn and the average and maximum velocities are $34km/h$ and $65km/h$ respectively. The initial position is perfectly known.

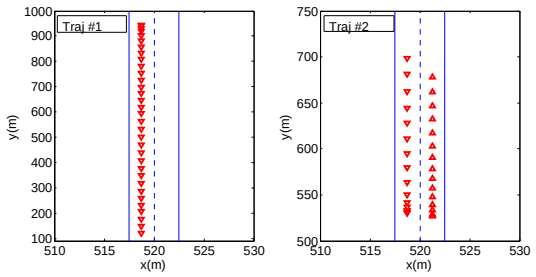

Fig. 2. The two traveled trajectories.

For the shadowing, the correlation function is the exponential one given by equation (28) with $\gamma = \ln(2)/dcorr$ and $dcorr = 50m$. The standard deviation of the shadowing is $\sigma_{sh} = 8dB$. The cross-correlation coefficient is equal to 0.5 and the coefficients of (10) are $\alpha = \beta = \sigma_{sh}/\sqrt{2}$.

The Macro-cell system simulation baseline parameters defined in [12] are used to compute the path loss as a function of the UE position. The UE makes measurements with 4 base stations located at $[0, 0]^T$, $[1391, 1032]^T$, $[-199, 1721]^T$ and $[1589, -688]^T$. The measurement error vector is white in time and Gaussian and has a covariance matrix $E\{\mathbf{n}_k \mathbf{n}_k^T\}$,

with $E\{n_{j,k}^2\} = 9dB^2$, $E\{n_{i,k}n_{j,k}\} = 0$ if the two error components correspond to different base stations and $E\{n_{i,k}n_{j,k}\} = 4.5dB^2$ if they correspond to different sectors of the same base station.

In Fig. 3, the RMSE of the position is plotted vs time for trajectory 1 and for a time step $T = 0.4$ seconds (s). These results are obtained by means of Monte Carlo simulations for 10 different sets of shadowing maps and for 50 trials per set, where a set represents the shadowing maps attributed to the different base stations. The Dead Reckoning (DR) curve corresponds to the estimation of the position based on the previous estimation and the acceleration only. In this case the position error is accumulated over time. A great improvement can be observed when the RB particle filter is used. Here, the order-1 AR is optimal since the trajectory is collinear, but the higher order AR simulation are not degraded. For the sake of illustration, the RMSE curves when the shadowing is perfectly known and when the shadowing is white are also drawn. We see that tracking the shadowing improves the RMSE, but the remaining imprecisions does not allow to remove its effect.

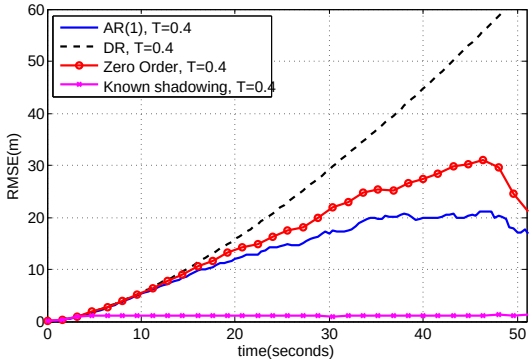

Fig. 3. RMSE of the position for trajectory 1. The time step is $T = 0.4$ s.

For trajectory 2, the time step is $T = 1$ seconds and the total duration is 30 seconds. Thus, an order equal to 30 is capable of taking into account all previous states. Fig. 4 shows the RMSE for this trajectory. After $t = 16$ seconds, when the turning occurs, the RMSE of $AR(10)$ and $AR(30)$ is lower than for $AR(1)$. Indeed, the adjacency of the two parts of the trajectory improves the estimation that exploits the shadowing correlation. Few seconds after, the RMSE of $AR(10)$ increases. This is explained by the fact that the AR order is not sufficient to exploit the shadowing correlation in the actual measurements and in the measurements obtained at the beginning of the trajectory. By exploiting previous measurements, the location tracking can be highly improved. Further improvement can be obtained from the a priori information brought by a fingerprinting map of the shadowing.

VII. Conclusions

In this paper, we introduced the auto-regressive modeling of the temporal evolution of the shadowing. We used this model to implement the Rao-Blackwellized particle filter, where we took the shadowing as a part of the state vector. To exploit

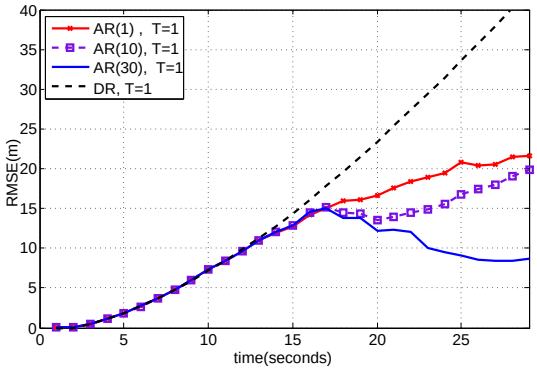

Fig. 4. RMSE of the position for trajectory 2 and for different AR orders. The time step is $T = 1$ s.

all the previous measurements, the order of the AR model increases with time, which involves increasing complexity and memory needs. This order can be limited according to several factors, such as complexity and memory limitations, the a priori knowledge of the itinerary, the map constraints, the update time step or the accuracy of INS information. We have shown the application to the particular case of straight trajectories, which is relevant for train position estimations, or map-based car navigation system.

VIII. Acknowledgement

This work has been performed in the framework of the ICT-248894 WHERE2 project funded by the European Union.

References

[1] Guolin Sun, Jie Chen, Wei Guo, and K.J.R. Liu. Signal processing techniques in network-aided positioning: a survey of state-of-the-art positioning designs. *Signal Processing Magazine, IEEE*, 22(4):12 – 23, july 2005.

[2] Theodore Rappaport. *Wireless Communications: Principles and Practice*. Prentice Hall PTR, Upper Saddle River, NJ, USA, 2001.

[3] M. Gudmundson. Correlation model for shadow fading in mobile radio systems. *Electronics Letters*, 27(23):2145 –2146, 7 1991.

[4] Kai-Jie Yang and Yuh-Ren Tsai. Location tracking in mobile networks under correlated shadowing effects. In *Wireless Communications and Networking Conference, 2009. WCNC 2009. IEEE*, pages 1 –5, 2009.

[5] Julien Guillet and Francois LeGland. Using noisy georeferenced information sources for navigation and tracking. In *Nonlinear Statistical Signal Processing Workshop, 2006 IEEE*, pages 156 –159, 13-15 2006.

[6] Arnaud Doucet. On sequential simulation-based methods for bayesian filtering. Technical report, 1998.

[7] F. Gustafsson, F. Gunnarsson, N. Bergman, U. Forssell, J. Jansson, R. Karlsson, and P.-J. Nordlund. Particle filters for positioning, navigation, and tracking. *Signal Processing, IEEE Transactions on*, 50(2):425 –437, feb 2002.

[8] T.B. Sorensen. Slow fading cross-correlation against azimuth separation of base stations. *Electronics Letters*, 35(2):127 –129, jan. 1999.

[9] Hugh Durrant-Whyte and Tim Bailey. Simultaneous localisation and mapping (slam): Part i the essential algorithms. *IEEE ROBOTICS AND AUTOMATION MAGAZINE*, 2:2006, 2006.

[10] H. Rue and L. Held. *Gaussian Markov Random Fields: Theory and Applications*, volume 104 of *Monographs on Statistics and Applied Probability*. Chapman & Hall, London, 2005.

[11] M. McGuire, K. N. Plataniotis, and A. N. Venetsanopoulos. Environment and movement model for mobile terminal location tracking. *Wirel. Pers. Commun.*, 24(4):483–505, 2003.

[12] 3GPP. Tr 25.814, physical layer aspects for evolved universal terrestrial radio access (utra) (release 7). September 2006.